Finding core-collapse supernovae from the epoch of reionization behind cluster lenses

Monthly Notices
of the
ROYAL ASTRONOMICAL SOCIETY

MNRASL **435,** L33–L37 (2013) doi:10.1093/mnrasl/slt089
Advance Access publication 2013 July 30

Finding core-collapse supernovae from the epoch of reionization behind cluster lenses

Tony Pan★ and Abraham Loeb

Harvard–Smithsonian Center for Astrophysics, 60 Garden Street, Cambridge, MA 02138, USA

Accepted 2013 July 3. Received 2013 June 26; in original form 2013 March 27

ABSTRACT

Current surveys are underway to utilize gravitational lensing by galaxy clusters with Einstein radii > 35 arcsec in the search for the highest redshift galaxies. Associated supernovae from the epoch of reionization would have their fluxes boosted above the detection threshold, extending their duration of visibility. We predict that the *James Webb Space Telescope (JWST)* will be able to discover lensed core-collapse supernovae at redshifts exceeding $z = 7$–8.

Key words: gravitational lensing: strong – supernovae: general – galaxies: clusters: general – early Universe.

1 INTRODUCTION

Clusters of galaxies act as gravitational lenses, focusing light rays from sources behind them and magnifying their images. As this effect enables observers to probe higher redshifts than ever probed before, surveys are being conducted with the *Hubble Space Telescope* (*HST*) to obtain deep images of the sky through massive galaxy clusters. One such ongoing programme is the Cluster Lensing And Supernova survey with Hubble (CLASH), which is imaging 25 clusters each to a depth of 20 orbits (Postman et al. 2012). The five clusters selected for this programme have large Einstein radii of 35–55 arcsec, maximizing their potential for discovering ultrahigh-redshift galaxies. Indeed, three candidate galaxies at redshifts $z \approx 9$–10 and another candidate galaxy at $z \approx 11$ have already been found in the CLASH fields (Bouwens et al. 2012; Coe et al. 2013). Similarly, the planned HST Frontier Fields[1] programme will target six strong-lensing galaxy clusters to reveal yet higher redshift galaxies.

The *James Webb Space Telescope* (*JWST*), the successor to *HST*, scheduled for launch in 2018, is likely to have analogous observational programmes with comparable integration times on a similar number of lensing clusters. Although the CLASH survey does aim to detect Type Ia supernovae (SNe) out to redshifts of $z \sim 2.5$, the current *HST* cluster observations are unlikely to detect gravitationally lensed SNe from the epoch of reionization at $z > 6$. Indeed, transient science was not identified as a science priority for the Frontier Fields programme, which will not revisit the same field twice. The greater sensitivity of *JWST* and its optimization for observations in the infrared could potentially allow it to find lensed SNe from the cosmic dawn in these same cluster fields.

The feasibility of finding gravitationally magnified SNe from $z \sim 1$–2 behind massive cluster lenses has already been demonstrated (Porciani & Madau 2000; Sullivan et al. 2000; Gal-Yam, Maoz & Sharon 2002; Stanishev et al. 2009), but the possibility of finding relatively faint SNe from the epoch of reionization via lensing has not been explored in detail. Observations of core-collapse SNe at $z > 6$ could help constrain the mass function of the stellar population responsible for ionizing the Universe (Pan, Kasen & Loeb 2012), and probe the history of reionization (Mesinger, Johnson & Haiman 2006).

In this Letter, we estimate the cosmic star formation rate during the epoch of reionization by requiring that enough Population II stars were formed to ionize the universe. Using model spectral time series for Type II SNe, as well as a simple isothermal sphere model for lensing, we calculate in Sections 2– 5 the required magnification and duration of detectability of such SNe at $z > 6$ for different *JWST* bands and integration times. Combining the above, we derive the snapshot rate, i.e. the expected number of gravitationally lensed core-collapse SNe detected in the field of view of *JWST* around these high-magnification clusters.

2 STAR FORMATION AND SUPERNOVA RATE

We infer the volumetric SN rate $R_{\rm SN}(z)$ as a function of redshift by relating it to the cosmic star formation rate density (SFRD) $\dot{\rho}_*(z)$:

$$R_{\rm SN}(z) = \dot{\rho}_*(z)\eta_{\rm SN} \approx \dot{\rho}_*(z)\frac{\int_{M_{\rm min}}^{M_{\rm max}} \psi(M)\,{\rm d}M}{0.7\int_{0.1}^{150} M\,\psi(M)\,{\rm d}M}, \quad (1)$$

where we use a Salpeter initial mass function (IMF), $\psi(M) \propto M^{-2.35}$, and include a factor of 0.7 in the mass integral to account for the shallower slope at $M \lesssim 0.5\,{\rm M}_\odot$ in a realistic IMF (Fukugita, Hogan & Peebles 1998). For the stellar mass range between $M_{\rm min} = 8$ and $M_{\rm max} = 40\,{\rm M}_\odot$ appropriate for optically-luminous core-collapse

★ E-mail: span@physics.harvard.edu
[1] http://www.stsci.edu/hst/campaigns/frontier-fields/

SNe, the conversion coefficient between the star formation rate and the SN rate is $\eta_{\rm SN} \sim 0.0097\,{\rm M}_\odot^{-1}$.

We require that enough massive stars were formed by the end of reionization so as to produce sufficient ionizing ultraviolet (UV) radiation to ionize the intergalactic medium by $z_{\rm end} = 6$. This follows the approach used in Pan et al. (2012), albeit with different parameters to bring our estimates closer to other inferences in the literature, as detailed below. The star formation rate during reionization peaks at late times, when metals expelled from a prior generation of star formation enriched the interstellar gas, so we assume that early Population II stars ($Z = 0.02\,{\rm Z}_\odot$) with a present-day IMF dominated the ionizing photon budget. Using the stellar ionizing fluxes of Schaerer (2002), we find the average number of ionizing photons produced per baryon incorporated into a Population II star was $\bar{\eta}_\gamma = 5761$. Thus, the mass in stars per comoving volume $\rho_*(z)$ should satisfy

$$\rho_*(z_{\rm end})\,\bar{\eta}_\gamma\ f_{\rm esc} = C\,\rho_{\rm b}, \tag{2}$$

where C is the number of ionizing photons necessary to ionize each baryon after accounting for recombinations, $\rho_{\rm b}$ is the cosmic baryon density and $f_{\rm esc}$ is the average escape fraction of ionizing photons from their host galaxies into the intergalactic medium. Also, we can relate the mass in stars per volume $\rho_*(z)$ to the mass in virialized haloes per volume via a star formation efficiency f_*:

$$\rho_*(z) = f_*\,\frac{\Omega_{\rm b}}{\Omega_{\rm M}}\int_{M_{\rm min}}^{\infty} M\,\frac{{\rm d}n(z)}{{\rm d}M}\,{\rm d}M, \tag{3}$$

where we use the Sheth–Tormen mass function of haloes for ${\rm d}n/{\rm d}M$ (Sheth & Tormen 1999), and $M_{\rm min} \sim 10^8\,{\rm M}_\odot$ is the minimum halo mass with atomic hydrogen cooling. The cosmological parameters, such as the matter and baryon densities, $\Omega_{\rm M}$ and $\Omega_{\rm b}$, were taken from Planck Collaboration et al. (2013). Assuming f_* is constant, we can calibrate f_* via equations (2) and (3), and then evaluate $\rho_*(z)$ at any redshift. The star formation rate is simply, ${\rm d}\rho_*(z)/{\rm d}t$.

Fig. 1 shows our estimated SFRD, with $C = 3$ and $f_{\rm esc} = 0.2$, resulting in an SFRD $\approx 2 \times 10^{-2}\,{\rm M}_\odot\ {\rm yr}^{-1}\ {\rm Mpc}^{-3}$ (comoving) between redshifts of $z = 6$ and 8. This corresponds to volumetric rates of approximately $2 \times 10^{-4}\ {\rm yr}^{-1}\ {\rm Mpc}^{-3}$ for core-collapse SNe. Our simple SFRD model and the resulting SN rates linearly scale with C and $f_{\rm esc}^{-1}$, so the *JWST* snapshot rates calculated later can be easily scaled for different parameter choices of the SFRD.

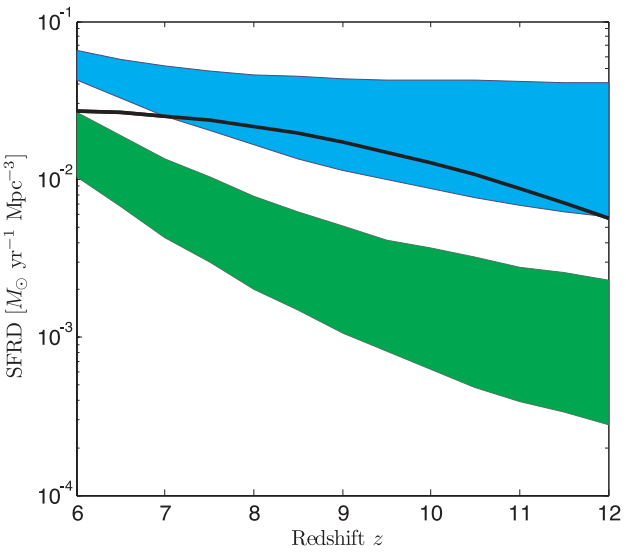

Figure 1. SFRD at high redshift. The black line shows our fiducial SFRD model used in later calculations. For comparison, the blue and green regions are taken from Robertson & Ellis (2012). The blue region (top) spans the high and low values for parametrized star formation histories consistent with gamma-ray burst (GRB) derived star formation rates, whereas the green region (bottom) denotes the SFRD histories derived from UV galaxy luminosity densities observed at high redshift, integrated down to the observation magnitude limit of $M_{\rm AB} \approx -18$. Note that the latter SFRD is likely to be significantly lower than the true cosmic SFRD, as the steep faint-end slopes of lower luminosity galaxies (possibly down to $M_{\rm AB} \lesssim -10$) are omitted (Ellis et al. 2013; Robertson et al. 2013), while the GRB-derived SFRD is much less flux limited and likely more accurate. Our SFRD parameters ($C = 3$ and $f_{\rm esc} = 0.2$) were chosen conservatively to be consistent with the low end of the GRB-derived SFRD.

3 LIGHT CURVES

We adopt the spectral time series of a Type II plateau SN from a red giant progenitor with an initial mass $15\,{\rm M}_\odot$, computed by Kasen & Woosley (2009) using a code that solves the full multiwavelength time-dependent radiative transfer problem. We plot the SN light curves in the observer frame for the best possible *HST* and *JWST* filters in Fig. 2. Note that Type II SNe are diverse transients with peak luminosities that can vary by more than an order of magnitude, and the relationship between the progenitor mass and the brightness of the SN is uncertain; we adopt a single characteristic model to represent all core-collapse SNe for the sake of simplicity. Type IIP SNe are the most common events, and the model light curves and spectra used here agree very well with observed SNe of average luminosities.

We verified that *HST* is, in practice, incapable of detecting a core-collapse SN from the epoch of reionization. The sensitivity of the *HST* 1.6 μm filter is only a factor of 2 worse than the *JWST F444W* filter, but its overwhelming drawback is its waveband, which can only probe the SN rest-frame UV flux at $z \geq 4$. Although the *JWST F356W* band is more sensitive, the *F444W* band will be optimal for detecting the highest redshift SN that gravitational lensing could provide. Fig. 3 shows the magnification necessary to detect Type II SNe at high redshifts for different integration times. Even with a 10^5 s exposure, a large magnification factor of $\mu \geq 10$ will be necessary for detecting Type IIP SNe at $z > 10$ with *JWST*.

4 LENSING MAGNIFICATION

For simplicity, we adopt a *singular isothermal sphere (SIS)* model for the mass distribution of the lensing cluster, within which the magnification properties are uniquely specified by the Einstein radius $\theta_{\rm E}$ (Schneider, Ehlers & Falco 1992). We denote the angular separations of the source and the image from the centre axis of the lens as β and θ, respectively. If the source lies within the Einstein radius $\beta < \theta_{\rm E}$, two images are created at locations $\theta_\pm = \beta \pm \theta_{\rm E}$, with magnifications $\mu_\pm = 1 \pm \theta_{\rm E}/\beta$. Note that μ_- has negative magnification, that is, the image is flipped compared to the source. If the source lies outside the Einstein radius $\beta > \theta_{\rm E}$, there is only one image at $\theta = \theta_+$ with magnification $1 < \mu_+ < 2$. We conservatively consider only the higher magnification image at θ_+, for which the source angle $\beta = \theta_{\rm E}/(\mu - 1)$.

Then, the differential source volume (comoving) of magnified events as a function of magnification and redshift is

$${\rm d}V(z, \mu) = {\rm d}A(z, \mu)\,{\rm d}D_{\rm C}, \tag{4}$$

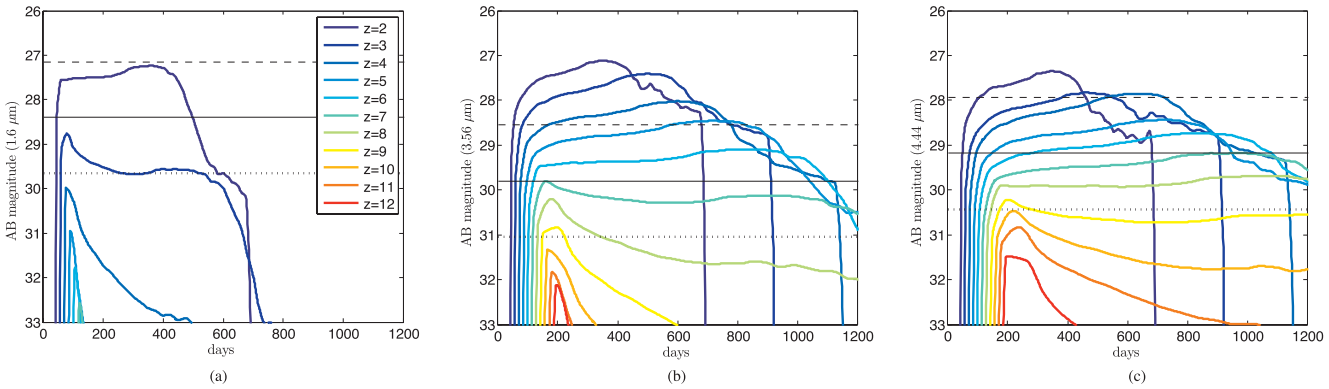

Figure 2. Observer-frame light curves for a Type IIP SN from a 15 $M_\odot$ red giant progenitor, for the *HST* Wide Field Camera-3 1.6 μm filter, and the *JWST* Near Infrared Camera (NIRCam) *F356W* and *F444W* wideband filters at 3.56 and 4.44 μm, respectively. The dashed, full and dotted horizontal lines denote the AB magnitude limits for a 10σ detection with 10^4, 10^5 and 10^6 s integration times, respectively, for each filter (corresponding to the flux limits 50, 13.8, 24.5 nJy, respectively, for 10^4 s exposures). Even a *Hubble Deep Field* measurement has no hope of seeing a regular Type II SN at $z \geq 6$. A 10^5 s exposure with *JWST* can detect a $z = 6$ SN without magnification. Gravitational lensing would extend its reach to higher redshifts and, more importantly, extend the duration for which the SN remains above the telescope detection threshold.

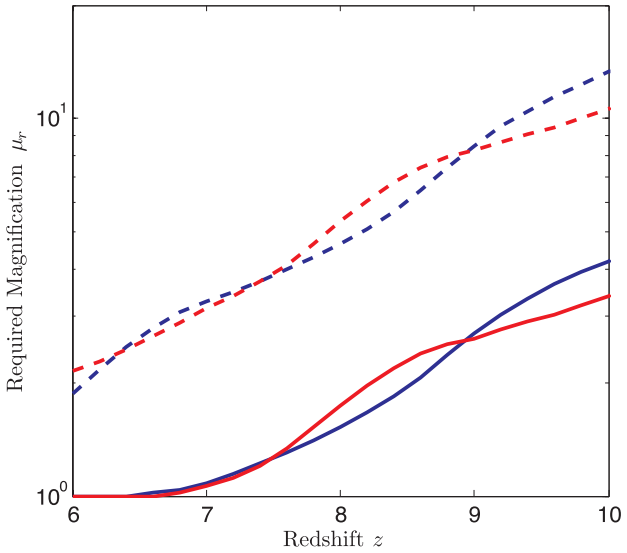

Figure 3. Required magnifications μ_r for detecting Type IIP SNe with *JWST* at high redshifts. The blue and red lines denote the results for the *JWST F356W* and *F444W* bands, respectively, while the dashed and solid lines correspond to integration times of 10^4 and 10^5 s. The latter integration time is similar to that used in CLASH.

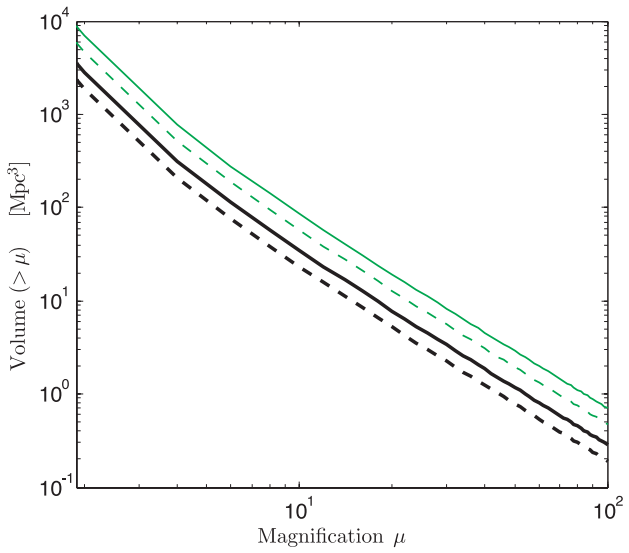

Figure 4. Comoving source volume as a function of magnification μ and redshift z over a redshift interval of $\Delta z = 1$ for an SIS lens. The black and green lines denote Einstein radii of 35 and 55 arcsec, respectively, while the solid and dashed lines denote $z = 6$ and 10, respectively. The results are in general agreement with more realistic estimates of the search areas per magnification factor for the magnification maps of the lensing clusters in the CLASH survey (Bouwens et al. 2012).

where the differential comoving distance $\mathrm{d}D_\mathrm{C}(z)$ is

$$\mathrm{d}D_\mathrm{C} = \frac{c}{H_0}\frac{1}{E(z)}\mathrm{d}z, \tag{5}$$

with $E(z) \approx \sqrt{\Omega_\mathrm{M}(1+z)^3 + \Omega_\Lambda}$, and the differential source area is

$$\begin{aligned}\mathrm{d}A(z,\mu) &= (2\pi\, D_\mathrm{A}(z)\beta\; D_\mathrm{A}(z)\mathrm{d}\beta\,)\,(1+z)^2 \\ &= \left(2\pi\frac{\theta_\mathrm{E}^2}{(\mu-1)^3}\mathrm{d}\mu\right) D_\mathrm{A}(z)^2(1+z)^2. \end{aligned}\tag{6}$$

Here $D_\mathrm{A}(z)$ is the angular diameter distance, and the extra $(1+z)^2$ is to adjust the area to comoving units. In Fig. 4, we plot the source volume for a range of Einstein radii typical of high-magnification clusters. Given core-collapse SN rates of $\sim 10^{-4}$ yr^{-1} Mpc^{-3}, capturing SNe with high magnifications within source volumes $< 10^2$ Mpc^3 is unlikely. Hence, we expect most lensed SNe detected to have their fluxes moderately boosted with $\mu \lesssim 5$; the benefit of lensing is to probe somewhat deeper redshifts, and to greatly extend the duration of visibility. Also, since high-redshift observations are background-limited, for a target signal-to-noise ratio, the limiting flux is proportional to $t^{-1/2}$, so even a modest magnification of $\mu \sim 3$ can reduce the required integration time by an order of magnitude.

This volume limitation of lensing also justifies our focus on core-collapse SNe which have the highest volumetric rates. Although Type Ia SNe are brighter, their volumetric rate is a factor of 4 smaller than the core-collapse rate at $z \approx 7$ (Pan et al. 2012), with the difference drastically increasing with redshift due to the long delay times needed between star formation and explosions for some

Type Ia events (Maoz, Mannucci & Brandt 2012). Pair-instability SNe from Population III stars have volumetric rates at least two orders of magnitude lower.

5 SNAPSHOT RATE

The snapshot 'rate' is the total number of events observed at a limiting flux within a given field (not per unit time). The differential snapshot rate can be calculated from equations (1) and (4) via

$$N(z, \mu)\, \mathrm{d}z\, \mathrm{d}\mu = R_{\rm SN}(z)\, t(F_\nu, \mu, z)\, \mathrm{d}V(z, \mu), \quad (7)$$

where $t(F_\nu, \mu, z)$ is the rest-frame duration over which an event with magnification μ will be brighter than the limiting flux F_ν at redshift z, for the observation wavelength ν under consideration. We find $t(F_\nu, \mu, z)$ using our spectral time series for the Type IIP SN model described in Section 3. As we care about the apparent SN rate for observers, there is an implicit factor of $(1 + z)^{-1}$ in front of the intrinsic volumetric SN rate $R_{\rm SN}(z)$, but that cancels with a $(1 + z)$ factor for $t(F_\nu, \mu, z)$ due to cosmic time dilation.

In Fig. 5, we plot the expected snapshot rate of magnified core-collapse SNe detected by *JWST* above target redshifts, calculated by integrating equation (7) over μ and partially over z. Since NIRCam has two modules each with a 2.2×2.2 arcmin^2 field of view, we limit the source area in equation (4) to images that lie within this field of view.

We find that a 10^5 s *JWST* snapshot with the *F444W* filter is expected to detect $\sim$1 magnified core-collapse SN at $z > 7$ around each cluster, and $\sim$0.1 SN at $z > 8$. Using approximately five clusters with $\theta_{\rm E} \geq 35$ arcsec, the prospects for detecting a few non-superluminous SNe at high redshifts via lensing are high. If the other $\sim$20 galaxy clusters in the CLASH survey with smaller Einstein radii of $\theta_{\rm E} \sim 15$–30 arcsec are also included, the expected number of gravitationally lensed high-z SNe detected should double.

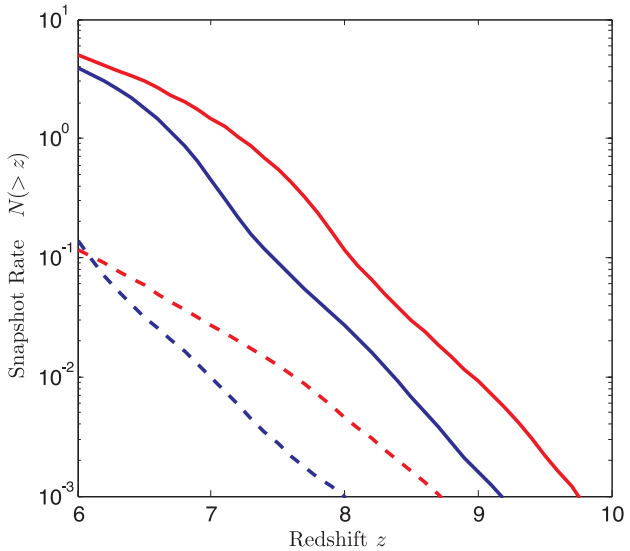

Figure 5. The snapshot rate of gravitationally lensed core-collapse SNe with *JWST*, for a *single* SIS lens with an Einstein radius $\theta_{\rm E} = 35$ arcsec. The line colour/dash scheme is the same as Fig. 3. Despite the higher sensitivity of the *F356W* band, the *F444W* band is better for finding lensed SNe at $z > 6$, as the SNe remain above the flux limit for a longer time. Note that five to six high-magnification galaxy clusters with $35 \leq \theta_{\rm E} \leq 55$ arcsec are targeted in strong-lensing surveys such as CLASH and HST Frontier Fields.

6 DISCUSSION

At $z > 6$, the observed duration of gravitationally lensed core-collapse SNe can reach $\gtrsim$1 yr, lending their detection to a search strategy of taking images separated by $\sim$0.5–1 yr, and looking for flux differences between consecutive snapshots. Ideally, the cluster survey should cover most of the critical curve area, and not just known locations of magnified images of high-z galaxies, as the lensed SN may appear in currently 'dark' critical curve areas, and serve as a flag for its fainter host galaxy. The spectral energy distribution of Type II SNe is sufficiently different from that of the blackbody to allow for photometric redshift determination; however, typing the SNe accurately may require time-consuming spectroscopy.

Our quantitative results improve upon previous calculations of the frequency of lensed SNe. For example, Marri, Ferrara & Pozzetti (2000) first explored the effects of gravitational lensing on high-z Type II SNe by intervening cosmological mass for different cosmologies, but the predicted detection rates were unrealistically high because of optimistic assumptions about *JWST* capabilities. Gunnarsson & Goobar (2003) explored the lensing by massive clusters of distant Type Ia and Type II SNe observed at wavelengths of 0.8–1.25 μm, but found the discovery rate tapered off at $z \sim 3$. Also, gravitational lensing is not required per se to detect Type II SNe from the epoch of reionization. A moderate *JWST* blank-field survey can obtain similar snapshot rates, albeit trading off the highest redshift events for more lower redshift ones compared to a lensing survey. For example, Mesinger et al. (2006) found that a 10^5 s exposure with *JWST* can detect 4–24 SNe per field at $z > 5$, although the assumed SFRD $\sim 0.1\,{\rm M}_\odot\ {\rm yr}^{-1}\ {\rm Mpc}^{-3}$ was an order of magnitude higher than our estimates here, and the current specifications for *JWST* NIRCam filter sensitivities are now approximately three times worse than the values assumed at that time.

We assumed a single peak magnitude for Type II SNe in our calculations. More realistically, the luminosity function of Type II SNe roughly resembles a Gaussian, with an average absolute magnitude of 16 ($\sigma = 1.4$), at least in the local universe (Li et al. 2011). As this is not a power-law distribution, there is no magnification bias in the usual sense, and it is unlikely to observe highly magnified Type II SNe with below average intrinsic luminosities. However, for Type II SNe brighter than $M_{\rm AB} = 16$, the luminosity function is steep. Hence, for observations that miss the average luminosity members of the Type II SN population at $z > 7$ (10^5 s or shorter exposures with *JWST*), lensing can increase the number of SNe detected.

For more luminous SNe, Whalen et al. (2013a) found that core-collapse SNe from Population III progenitors in the earliest galaxies could be visible with the deepest *JWST* surveys (reaching $M_{\rm AB} = 32$) even at $z > 10$, as these SNe are bluer and almost an order of magnitude brighter than the average Type II SNe considered in this Letter. Whalen et al. (2013b) also found that superluminous Type IIn SNe powered by circumstellar interactions from Population III stars could be visible out to $z \sim 20$. Truly massive Population III stars with masses $M \gtrsim 200\,{\rm M}_\odot$ can also die as extremely-bright pair-instability SNe, detectable with *JWST* at $z > 15$ (Hummel et al. 2012; Pan et al. 2012); indeed, the current record for the highest-redshift SN ever observed is likely a pair-instability or pulsational pair-instability event at $z = 3.90$ (Cooke et al. 2012). However, the small volumetric density of Population III stars makes it unlikely that these events will be strongly lensed. Finally, there is growing evidence of a prompt population of Type Ia SNe, so their volumetric rates during the later stages of reionization may not be negligible.

With the fiducial SFRD model in this Letter, we estimate $\gtrsim$1 gravitationally lensed Type Ia SNe could be discovered at $z > 7$ in the snapshots across the approximately five high-magnification clusters at any given time.

At lower redshifts, the measured core-collapse SN rate is a factor of $\sim$2 lower than that predicted from the cosmic star formation rate (Horiuchi et al. 2011); the most likely explanation is that some SNe are dim, whether intrinsically faint or due to dust obscuration. This will reduce our predicted snapshot rate. However, we ignored the contribution of multiple lensing images in our analysis. Due to the gravitational lens time delay, which could be $\sim$1–100 yr for strong lensing around the clusters of interest (Coe et al. 2013), multiple images arriving at different times can increase the expected snapshot detection rate of separate SNe within the same field of view. Although our SIS lens model can produce a maximum of only two magnified images, substructure and ellipticity in actual galaxy clusters will likely increase both the number of images and their magnifications. Scaling off the number of image systems around CLASH clusters, the inclusion of ellipticity would increase our estimated number of lensed SN images by $\sim$50 to 100 per cent (Zitrin et al. 2011, 2013).

ACKNOWLEDGEMENTS

We are grateful to Dan Kasen for providing the spectral time-series data for the Type IIP SN model used in this Letter. TP was supported by the Hertz Foundation and the National Science Foundation via a graduate research fellowship. This work was supported in part by NSF grant AST-0907890 and NASA grants NNX08AL43G and NNA09DB30A.

REFERENCES

Bouwens R. et al., 2012, preprint (arXiv:e-prints)
Coe D. et al., 2013, ApJ, 762, 32
Cooke J. et al., 2012, Nat, 491, 228
Ellis R. S. et al., 2013, ApJ, 763, L7
Fukugita M., Hogan C. J., Peebles P. J. E., 1998, ApJ, 503, 518
Gal-Yam A., Maoz D., Sharon K., 2002, MNRAS, 332, 37
Gunnarsson C., Goobar A., 2003, A&A, 405, 859
Horiuchi S., Beacom J. F., Kochanek C. S., Prieto J. L., Stanek K. Z., Thompson T. A., 2011, ApJ, 738, 154
Hummel J. A., Pawlik A. H., Milosavljević M., Bromm V., 2012, ApJ, 755, 72
Kasen D., Woosley S. E., 2009, ApJ, 703, 2205
Li W. et al., 2011, MNRAS, 412, 1441
Maoz D., Mannucci F., Brandt T. D., 2012, MNRAS, 426, 3282
Marri S., Ferrara A., Pozzetti L., 2000, MNRAS, 317, 265
Mesinger A., Johnson B. D., Haiman Z., 2006, ApJ, 637, 80
Pan T., Kasen D., Loeb A., 2012, MNRAS, 422, 2701
Planck Collaboration et al., 2013, preprint (arXiv:e-prints)
Porciani C., Madau P., 2000, ApJ, 532, 679
Postman M. et al., 2012, ApJS, 199, 25
Robertson B. E., Ellis R. S., 2012, ApJ, 744, 95
Robertson B. E. et al., 2013, ApJ, 768, 71
Schaerer D., 2002, A&A, 382, 28
Schneider P., Ehlers J., Falco E. E., 1992, Gravitational Lenses. Springer, New York
Sheth R. K., Tormen G., 1999, MNRAS, 308, 119
Stanishev V. et al., 2009, A&A, 507, 61
Sullivan M., Ellis R., Nugent P., Smail I., Madau P., 2000, MNRAS, 319, 549
Whalen D. J., Joggerst C. C., Fryer C. L., Stiavelli M., Heger A., Holz D. E., 2013a, ApJ, 768, 95
Whalen D. J. et al., 2013b, ApJ, 768, 195
Zitrin A. et al., 2011, ApJ, 742, 117
Zitrin A. et al., 2013, ApJ, 762, L30

This paper has been typeset from a TEX/LATEX file prepared by the author.